Detection of delamination onset in laser-cut carbon fiber transverse crack tension specimens using acoustic emission

Torben Prieß[1], Markus GR Sause[2], Daniel Fischer[1] and Peter Middendorf[1]

Abstract

Numerous experimental studies have been made on cutting carbon fibers with lasers with the focus on productivity due to high cutting speeds. However, the laser-cutting process has an influence on the mechanical properties of the carbon fiber-reinforced plastic. This paper presents a test to determine the impact of thermal damage at the cutting edge. The initiation load for mode II delamination at the transverse crack tension test can be used to estimate the impact on the mechanical properties of thermal damage at the cutting edge. Detection of the initiation load is done via acoustic emission methods. Two different specimen geometries show a decrease of more than 40% of the initiation load for a CO_2 continuous wave laser system with a large heat-affected zone compared to mechanically cut specimens.

Introduction

In recent years, laser-cutting processes have become increasingly important for the production of components made out of carbon fibers. The advantage of the laser cutting is the wearless process with no acting force on the work piece. It is possible to cut carbon fiber fabrics, e.g. on a 3D preform in order to improve the draping behavior. In this case, the laser-cut edge stays in the final part out of carbon fiber-reinforced plastic (CFRP). Numerous researches have been done on the laser-cutting process on CFRPs[1,2] as well as on cutting carbon fibers.[3–6] In these studies, the focus is on high productivity due to high cutting speeds.

To cut carbon fibers, the material has to be vaporized since no liquid phase exists at ambient pressure. The sublimation temperature of carbon fibers is $\approx 3600°C$.[7] Concerning the quality of the cut, different phenomena have been reported. In all studies, the carbon fibers show a significant increase in diameter up to about 50%. This phenomenon is called "fiber-swelling". The reason for this behavior is not explored. Furthermore, a thermal fused edge is observed. All authors assumed that the fused edge stemmed from condensated carbon at the fibers resulting from the cutting process.

Voisey et al.[8] found that swelling extends to around 100 µm from the cut. Weber et al.[7] have reported that "fiber-swelling" at temperatures above $\approx 2700°C$ occurs over a distance of 370 µm. A dependency of the amount of diameter change is found from the type of fibers and therefore from the former heat treatment as well as the laser system used.[9] The temperature during manufacture of the fibers has an influence on the orientation of the graphite crystallites.[10]

Cheng et al.[11] have proposed that irreversible changes occur in the graphite structure due to the expansion of embedded gas pockets. Voisey et al.[8] reduced the fiber swelling by storing the fibers in an oven at 2000°C for 12 h in an argon atmosphere and

[1]Institute of Aircraft Design, University of Stuttgart, Pfaffenwaldring, Stuttgart, Germany
[2]Institute for Physics, University of Augsburg, Augsburg, Germany

Corresponding author:
Torben Prieß, Institute of Aircraft Design, University of Stuttgart, Pfaffenwaldring 31, 70569 Stuttgart, Germany.
Email: priess@ifb.uni-stuttgart.de

explain this behavior with a volatilization of impurities as well as structural changes in the fibers.

Meyer[6] have investigated infused laser-cut carbon fiber preforms with resin. The specimens had a quasi-isotropic layup. For a CO_2 continuous wave laser, the compression strength has been shown to decrease in comparison to coupons manufactured with preforms cut with a cutter. The reason for the decrease of the compression strength attributed to poor fiber/matrix bond at the fused laser-cut edge.[6]

To our knowledge, no further work on the impact of the laser-cut fibers on mechanical properties of fiber composites is to be found in the literature. One key challenge in this aspect is a reliable test method. The transverse crack tension (TCT) test is a commonly used test to characterize mode II delamination.[12–15] By this delamination, the quality of the fiber fiber/matrix interface can be estimated.[16,17] The specimen consists of unidirectional ply layers with one center ply cut transverse to the fiber direction (see Figure 1).

In principle, the same stress state can be measured with the more common end notched flexure (ENF) test. But the ENF-test is based on a precrack induced with a foil inside the specimen to measure the propagation of the delamination. With the TCT-test, it is possible to determine the initiation of the delamination.

During the TCT-test, a first crack occurs in the resin rich pocket between the cut fiber ends. At certain load (initiation stress), a "fuzzy" delamination starts around the cut followed by a major delamination that occurs at a propagation stress.[12,18] This is also indicated by a drop in the load. This propagation load is used for calculation of the mode II fracture energy. According to Cui et al.[12] and Wisnom,[18] the initiation stress occurs at 87% to 97% of the propagation stress. Figure 2 shows the different delamination steps for a glass fiber specimen.

For glass fiber specimens, the initiation stress is normally estimated via visual observation.[12,18] However, this method is not feasible for carbon fiber specimens since these are not transparent. One adequate alternative is the detection of the initiation stress via acoustic emission methods.

All microscopic failure mechanisms in fiber-reinforced materials result in rapid microscopic displacements. These microscopic displacements in turn cause an excitation of elastic waves in the ultrasonic frequency range. Using piezoelectric sensor systems, these transient acoustic signals can be detected and analyzed.

The measurement of these acoustic emission signals is frequently used to detect the onset and position of microscopic failure occurring in fiber-reinforced materials.[19–25] In recent years, many attempts have been made to distinguish between different types of failures in fiber-reinforced materials.[20–24,26] The acoustic emission analysis used in the present study follows a recently developed pattern recognition method to distinguish and quantify different failure mechanisms in carbon fiber-reinforced polymers.[27] The validity of the source identification by the proposed method is based on reference calculations of the acoustic emission source, signal propagation, and signal detection process by finite element modeling.[28–30] It is worth noting that

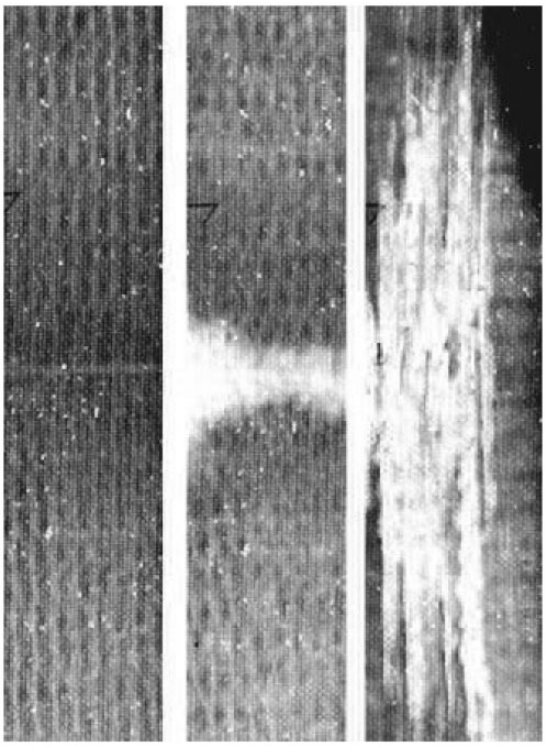

Figure 2. Fracture process of a TCT-specimen (glass fibers for visibility of the different fracture steps).

Figure 1. Layup of a transverse crack tension specimen.

Wilcox et al.[31] recently presented an analytical approach on the forward modeling of the acoustic emission process that shows similar predictive capabilities to validate source identification procedures. Since a comprehensive description of the methodological background is beyond the scope of the present study, we refer to the original publications[28–30] for a detailed review on the relations between source mechanisms and acoustic emission signal properties.

This paper presents a test method to estimate the influence of the laser-cutting process on the delamination onset of unidirectional carbon fibers. For TCT tests, the initiation load is estimated via acoustic emission analysis. The stress level for this delamination onset is investigated for specimens with laser and mechanically cut fibers.

Experimental procedures

Materials and laser system

For the tests, a unidirectional carbon fiber fabric out of Toray T700 50 C, 24 k is used. The fabric areal weight is 302 g/m^2, the content of carbon fibers is about 278 g/m^2.

The laser cutting of the discontinuous plies is done with the CO_2 continuous wave laser TruFlow5000 from Trumpf. The wavelength is $\lambda = 10,6\,\mu m$ (radially polarized), with $P = 1\,kW$ of power and a feed rate of $v = 3\,m/min$. The focal position is 4 mm above the fibers at a focal diameter of $df = 230\,\mu m$. In order to validate the test procedure, these parameters were chosen since they show a large fiber-swelling effect with an increase in diameter of approximately 100% at the cut edge. For the reference specimens, the discontinuous layers are cut manually with a cutter. Figure 3 shows the scanning electron micrographs of the cut edges from the laser and mechanically cut reference specimens.

Specimen preparation

Two different specimen types with three and five layers are tested to consider a possible influence of the specimen thickness as reported from Cui et al.[12] for the fracture energy. The two specimen types contain one cut ply and 2 respectively 4 continuous plies. The fibers are infused using a vacuum-assisted resin infusion process. A peel ply is used on both sides for a good adhesion of the tabs. The Momentive EPIKOTE™ Resin MGS® RIMR 135 is used with EPIKURE™ Curing Agent MGS® RIMH 1366. Curing is done over 24 h at room temperature followed by postcuring in an oven at 80°C for 15 h. The laminates have a fiber volume fraction between 59% and 62% (according to DIN EN 2564). The thickness is 1 mm (three layers) and 1.6 mm (five layers). The thickness of the laser-cut specimens is not measured in the area of the swollen fibers. After trimming the edges, glass fiber-reinforced plastic tabs with a thickness of 1.3 mm are glued with Larit A10–Larit B10. The specimens are cut with water-cooled diamonds saw to a width of 25 mm.

Figure 4 shows a photomicrograph of the two specimen types. The resin-rich region of the mechanically cut specimens is slightly larger compared to the laser-cut ones. The reason for this defect is a manufacturing imperfection in the lay-up process. Since the continuous layers show no undulation in the area of the resin-rich region, this has no influence on the resistance to delamination.[14] Due to the fiber swelling, the laser-cut specimens show an undulation of the continuous layers in the area of the laser cut.

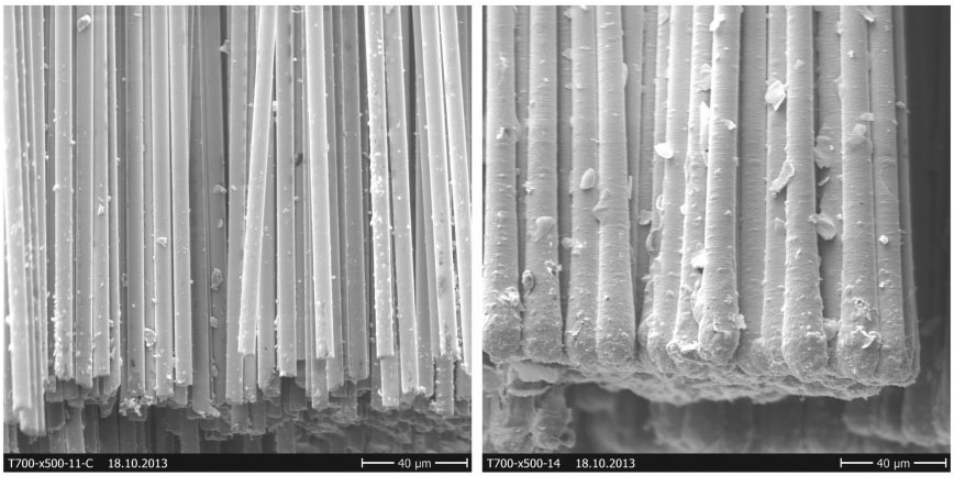

Figure 3. Scanning electron micrographs of the cut fibers with cutter (left) and laser (right).

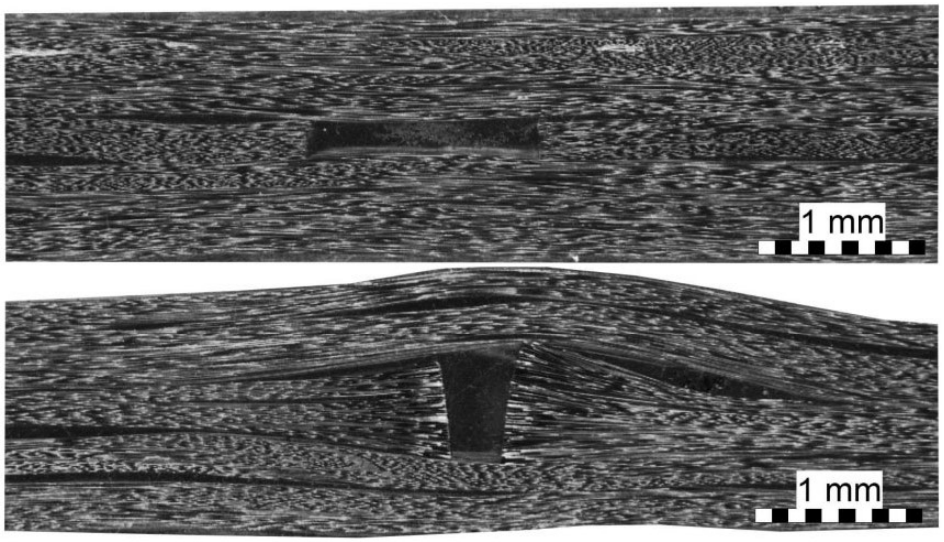

Figure 4. Photomicrograph of the TCT specimens (five layers) with cutter (above) and laser cuts (below).

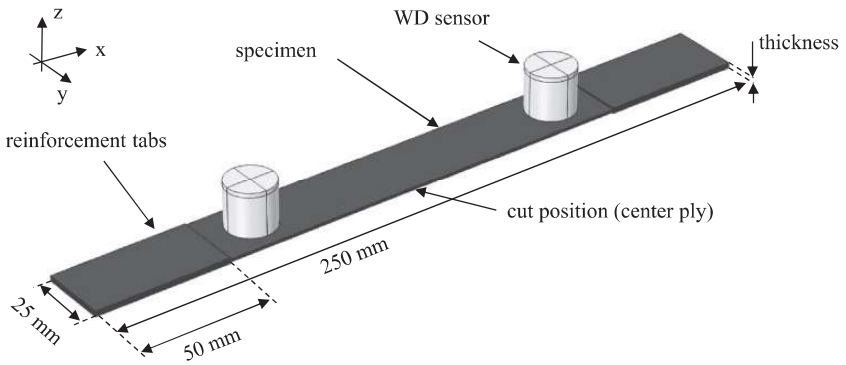

Figure 5. Specimen dimensions and arrangement of the acoustic emission sensors.

Mechanical testing

Testing is done using a universal testing machine Z250 from Zwick with a 250 kN load cell and displacement control at a rate of 1 mm/min. For visual monitoring of the strain field, an ARAMIS 12 M digital image correlation system was used. The field of view is located at the side surface of the specimen. Acquisition is done using 2D-measurements with a sampling rate of 2 Hz and an object distance of 47 mm.

Acoustic emission system

Acoustic emission (AE) signals were recorded using a Mistras PCI-2 system with 2/4/6 preamplifiers and two WD (wide band) AE sensors in linear arrangement as illustrated in Figure 5.

The signals were detected with a threshold-based triggering mechanism using 10/80/300 µs (Peak-Definition-Time/Hit-Definition-Time/Hit-Lockout-Time) at a threshold of 35 dB_{AE} and a preamplification of 20 dB_{AE}. The data were recorded with an acquisition rate of 10 MS/s and a band-pass filter ranging from 20 kHz to 1 MHz. An Event-Definition-Time of (15 ± 2) µs was used to avoid detection of signals from positions outside the range between the two sensors. Acoustic coupling was provided by a medium viscosity silicone grease. The sensors were attached using clamp systems to ensure a reproducible mounting pressure. Sensor coupling was validated by mutual pulsing of both sensors and comparison of the detected signal amplitudes. The sound velocity of the initial arrival of the fundamental symmetric Lamb wave mode is obtained from the measured time difference between the time of pulsing of sensor 1 and the arrival time at sensor 2 divided by their respective metric distance.

After signal acquisition, the acoustic emission source position was calculated by delta-t localization techniques using the one-dimensional sensor arrangement. For the application of the pattern recognition method,

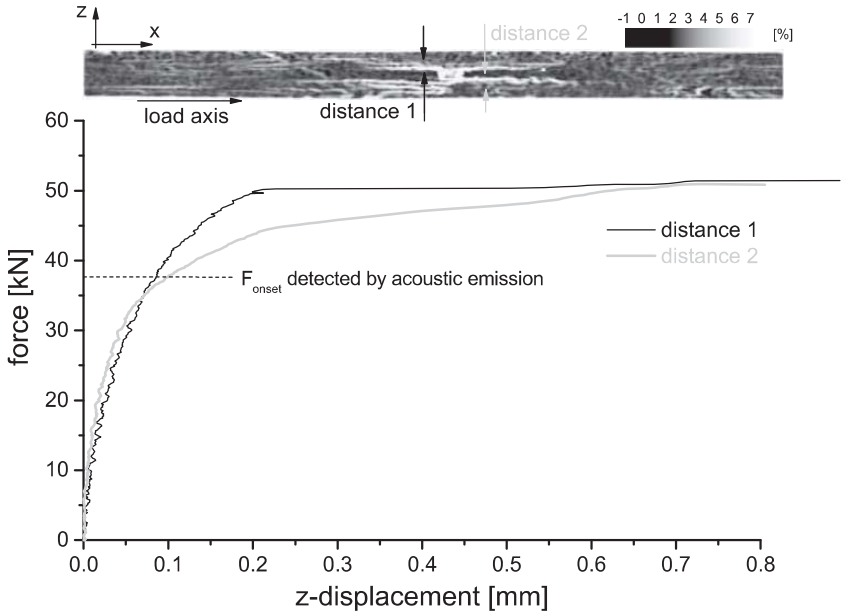

Figure 6. Exemplary evaluation of local–displacement values for one laser-cut specimen detection using digital image correlation.

the acoustic emission signal parameters (features) of both sensors were calculated from the first 100 µs of the signals after the signal arrival.

An application of the pattern recognition method described in Sause et al.[27] yields three signal classes for all 24 specimens investigated. Based on the method proposed in Sause and Horn,[32] the uncertainty of the classification was evaluated to be less than 0.20% for all specimens investigated. It is not part of the pattern recognition approach to correlate classes of acoustic emission signals to particular failure types. This can solely be achieved by secondary methods as compared to the acoustic emission source positions to microscopy results. An alternative approach is the comparison of the measured acoustic emission signals with respective signals obtained from finite element simulations as recently introduced in Sause and Horn.[28]

Results and discussion

In order to compare laser and mechanically cut specimens, three approaches were evaluated. First, a method to deduce the level of the propagation load, which is normally used for the quantification of mode II interlaminar fracture toughness[12,18] is applied. The evaluation shows only a small difference between the two cutting technologies. For the laser-cut specimens, the propagation load is about 13% (three layers) and 11% (five layers) lower than the reference coupons with mechanically cut fibers. At this load level, a small delamination around the cut fibers already exists. The size of the fiber swelling decreases with increasing distance from the cut. Therefore, the influence of the swelling on the delamination progress decreases with an increased distance to the cut edge. The estimation of the propagation load with the geometry used is slightly more subjective. In some cases, the specimens show a yielding effect with no clear drop in load.

A second approach, the local displacement field as obtained from the digital image correlation system was evaluated to measure the load corresponding to the first initiation of delamination. To obtain a quantitative measure of the strain field, the displacement in the through-thickness direction (z-displacement) was evaluated at several x-positions in the vicinity of the discontinuous center ply. The z-displacement was measured relative to the position of the center ply as indicated in the top image in Figure 6. An exemplary evaluation of the measured z-displacement of two lines is shown as a function of load in Figure 6. Since the position of the lines was chosen at arbitrary x-positions and no clear signature or mutual agreement in the shape of the individual curves was found, the optical detection of the delamination onset was found to yield unreliable results.

At the onset of the delamination, as detected by the acoustic emission (see below), no evident signature could be detected in the displacement field. This indicates that the initiation of delamination is not only a uniform process over the width of the TCT specimens but may also initiate within the specimen volume. Therefore, detection of the delamination onset based solely on information obtained at the specimen surface may be error prone.

The third method used acoustic emission signals. Based on previous results from tensile specimens,[29]

the detected acoustic emission signals could be assigned to the occurrence of matrix cracking, interfacial failure, and fiber breakage. This is based on their characteristic frequency spectra as validated by finite element simulation[28] and reported by various authors.[19–24] One representative classification result is shown in Figure 7.

Figure 8 shows a representative analysis result of a typical laser-cut specimen. With increased load, acoustic emission signals initiate at weak spots inside the laminate. Although the discontinuous center ply is intentionally designed as a weak spot, the first acoustic emission signals are localized at various positions along the x-axis of the specimen. Since these signals were classified as matrix cracks it is likely that they originate from failure at the specimen edges, failure at resin rich areas or failure at randomly distributed minor fabrication defects. At a distinct load level, signals classified as interfacial failure initiate specifically at the position of the discontinuous center ply ($x = 50$ mm).

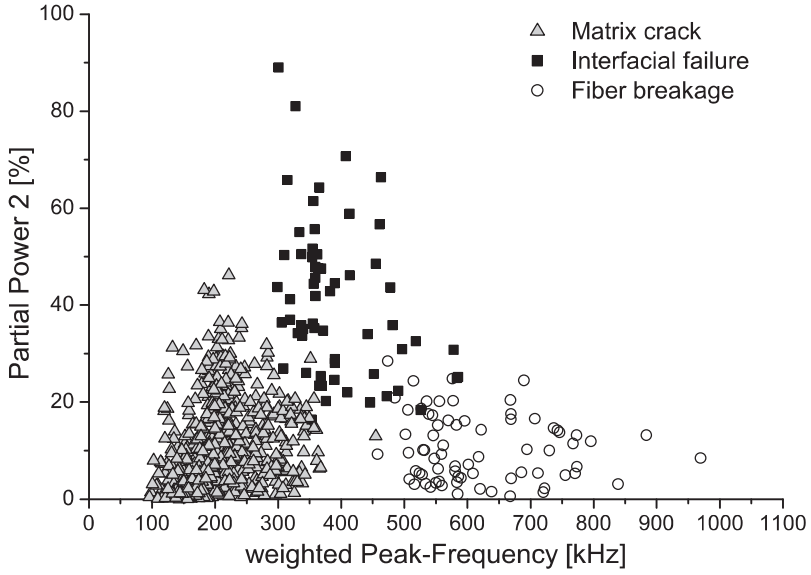

Figure 7. Exemplary classification result of pattern recognition process according to Sause et al.[27] The frequency for partial power 2 varies from f1 = 150 kHz and f2 = 300 kHz.

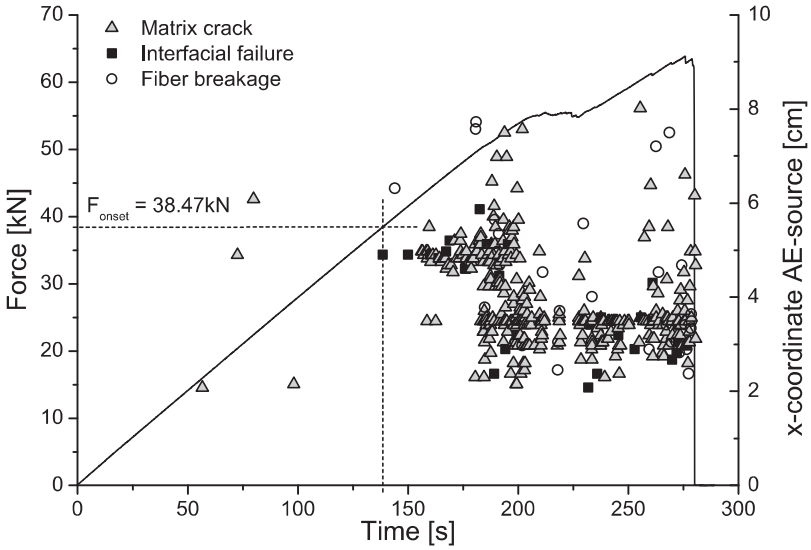

Figure 8. Force–time curve superimposed by x-coordinate of acoustic emission source position. The different symbol types reflect the type of failure as classified by the pattern recognition process.

Subsequently, acoustic emission signals are localized in the vicinity of the discontinuous center ply, which densify around $x = 50\,\text{mm}$ and spread outwards with increased load level. This is indicative of interlaminar crack growth, starting at the interrupted center ply. At increased load levels, acoustic emission signals are localized in a broad range between the two sensors. This is indicative of additional damage occurring at several positions inside the specimen. Among these signals, some are classified as fiber breakage signals. Since the tensile strength of carbon fibers typically shows Weibull-type distributions, failure of individual fiber filaments is quite likely before the ultimate load level of the laminate is reached.[33] Therefore, occurrence of sporadic single fiber breakage long before ultimate failure is a likely source for these acoustic emission signals.

Remarkably, the relevant acoustic emission signals occur long before significant signatures are visible in the load–displacement curves. Since the initiation of interfacial failure at the position of the discontinuous center ply is of key interest for further analysis, the load level of initiation was quantified by acoustic emission measurements. Therefore, the first occurrence (onset) of the acoustic emission signals, classified as interfacial failure within the range of the discontinuous center ply ($50 \pm 5\,\text{mm}$ x-coordinate) was used to obtain the respective load level of failure initiation.

The stress for onset of delamination and for propagation is shown in Table 1 for the two geometries tested. In comparison with the mechanically cut specimens, the onset of the delamination is about 41% (three layers) and 48% (five layers) lower for the laser-cut specimens. This indicates that the laser-cutting process has a negative influence on the mechanical properties of the CFRP.

Table 1. Comparison of the stress at first delamination for different geometries.

Cut plies	1	1	1	1
Continuous plies	2	2	4	4
Laser/cutter	Cutter	Laser	Cutter	Laser
Stress at onset of delamination (MPa)	897	527	1240	645
Standard deviation (MPa)	103	37	94	118
Stress at propagation load (MPa)	1130	979	1352	1196
Standard deviation (MPa)	130	79	44	54

The lower load level for the delamination can result from different effects. Due to the changed fiber surface (see Figure 3), the fiber/matrix interface is probably damaged compared to the original fibers. Furthermore, the lower delamination load can also result from the changed geometry and fiber waviness of the laser-cut specimens (see Figure 4) as well as due to a different local fiber volume fraction in the area of the swollen fiber.

Another possible source for the delamination is the molted stitching yarn of the carbon fiber fabric. The polyester yarn is not cut directly by the laser process since the laser energy is not absorbed by the polyester.[34] The yarn melts due to the heat transferred by the carbon fibers and remains as a slug at the end of the heat-affected zone in the fabric. The size and shape of the slugs are not constant, since the melting process of the polyester is not stable. Figure 9 shows a photomicrograph of a laser-cut TCT specimen with a stitching yarn slug.

The position corresponds to the size of the heat-affected zone, and therefore depends on the laser process. With different laser parameters, e.g. a pulsed laser system, the size of the heat affected zone can be strongly reduced. This leads to significantly smaller amount of melting polyester and the slug can be minimized or avoided.

All these possible effects follow from the laser-cutting process. Therefore, the laser process is the basic reason for the lower load level for the delamination onset.

Summary and conclusions

The influence of the laser-cutting process on the delamination onset of unidirectional carbon fibers is investigated. For TCT tests, the initiation load is estimated via acoustic emission analysis with consistent results.

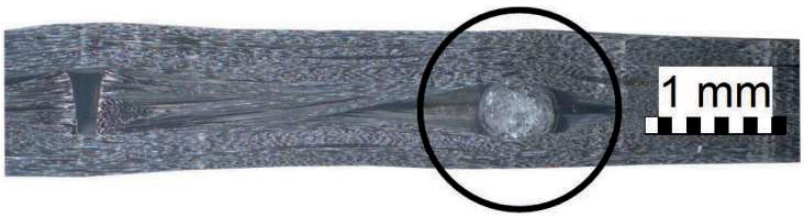

Figure 9. Photomicrograph of a laser-cut TCT specimen with a stitching yarn slug.

The onset of the delamination is about 41% (three layers) and 48% (five layers) lower for the laser-cut specimens compared to the mechanically cut reference specimens. The decrease for the propagation load is about 13% (three layers) and 11% (five layers) compared to the reference coupons.

The significantly lower initiation load for the laser-cut specimens indicates that this test method is suitable for the evaluation of the mechanical properties of laser-cut carbon fibers. Furthermore, the results show that the laser-cutting process has a negative influence on the mechanical properties of the CFRP. The reason for the lower onset of the delamination can be a changed fiber surface, the changed geometry of the fibres due to the "fiber-swelling" as well as the molted stitching yarn of the fabric. However, to validate the test procedure, the parameters of the laser system were chosen in order to produce a large "fiber-swelling" effect. With different laser parameters, e.g. a pulsed laser system, this effect could probably be strongly reduced.

The present results show that the initiation load of TCT tests can be used to estimate the effect of different changes of the fibers directly at the cutting edge.

Acknowledgments

The authors thank Michael Jarwitz from the IFSW Stuttgart for the laser-cut fibers, as well as Stefan Schmitt from theInstitute of Physics, University of Augsburg, for carrying out the TCT test and the DIC analysis.

Conflict of interest

None declared.

Funding

This work is part of the ProCaV-Projekt sponsored by the German Federal Ministry of Education and Research (FKZ: 13N11912).

References

1. Jung KW, Kawahito Y and Katayama S. Ultra-high speed disk laser cutting of carbon fiber reinforced plastics. *J Laser Appl* 2012; 24: 012007–1–012007–8.
2. Harada Y, Kawai K, Suzuki T, et al. Evaluation of cutting process on the tensile and fatigue strength of CFRP composites. In: Chandra T, Ionescu M and Mantovani D (eds) *Materials science forum* (Vols. 706–709). Switzerland: Trans Tech Publications, 2012, pp.649–654.
3. Fuchs AN, Schoeberl M, Tremmer J, et al. Laser cutting of carbon fiber fabrics. *Phys Procedia* 2013; 41: 365–373.
4. Hindersmann A, Malzahn S, Torstrick S, et al. Endkonturnahe Faserverbundbauteile durch hochgenaue Preform-Feinbesäumung mittels Lasertechnologie. In: *Deutscher Luft- und Raumfahrtkongress*. Bonn, Germany: DGLR. 2011, pp.493–502.
5. Klotzbach A, Vessio P, Klotzbach U, et al. Investigations in remote cutting of carbon fiber composite materials. In: *ICALEO: 30th international congress on applications of lasers & electro-optics*. Orlando, FL, USA: Laser Institute of America, 2011, pp.511–515.
6. Meyer O. Kurzfaser-Preform-Technologie zur kraftflussgerechten Herstellung von Faserverbundbauteilen. Institut für Flugzeugbau (IFB), Universität Stuttgart, 2008.
7. Weber R, Hafner M, Michalowski A, et al. Analysis of thermal damage in laser processing on CFRP. In: *ICALEO 2011*, Orlando, 2011.
8. Voisey KT, Fouquet S, Roy D, et al. Fibre swelling during laser drilling of carbon fibre composites. *Opt Laser Eng* 2006; 44: 1185–1197.
9. Prieß T, Hafner M, Weber R, et al. Influence of laser processing on carbon fibres. In: *Stuttgart laser technology (SLT) forum*, Stuttgart, 2012.
10. Morgan P. *Carbon fibers and their composites*. Boca Raton, FL, USA: CRC Press Taylor & Francis, 2005.
11. Cheng CF, Tsui YC and Clyne TW. Application of a three-dimensional heat flow model to treat laser drilling of carbon fibre composites. *Acta Materialia* 1998; 46: 4273–4285.
12. Cui W, Wisnom MR and Jones M. An experimental and analytical study of delamination of unidirectional specimens with cut central plies. *J Reinforc Plast Compos* 1994; 13: 722–739.
13. van der Meer FP and Sluys LJ. A numerical investigation into the size effect in the transverse crack tension test for mode II delamination. *Compos Part A: Appl Sci Manufact* 2013; 54: 145–152.
14. Prieto LL, Spenninger G and Wagner H. Experimental determination of energy release rate of Cfrp structures by means of transverse crack tension tests. In: Bos MJ (ed.) *ICAF 2009, Bridging the gap between theory and operational practice*. Netherlands: Springer, 2009, pp. 513–528.
15. Prinz R and Gaedke M. Characterisation of interlaminar mode I and mode II fracture in CFRP laminates. In: *Spacecraft structures and mechanical testing, Proc. Int. Conf. organised by the European Space Agency. ESA SP-321, ESTEC*, Noordwijk, the Netherlands, 1991, Noordwijk, The Netherlands: ESA Publications Division ESTEC, pp. 97–102.
16. Talreja R and Singh CV. *Damage and failure of composite materials*. Cambridge: Cambridge University Press, 2012.
17. Drzal LT, Herrera-Franco PJ and Ho H. 5.05 – Fiber matrix interface tests. In: Anthony Kelly E and Zweben C (eds) *Comprehensive composite materials*. Oxford: Pergamon, 2000, pp.71–111.
18. Wisnom MR. On the increase in fracture energy with thickness in delamination of unidirectional glass fibre-epoxy with cut central plies. *J Reinforc Plast Compos* 1992; 11: 897–909.
19. Surgeon M and Wevers M. Modal analysis of acoustic emission signals from CFRP laminates. *NDT & E Int* 1999; 32: 311–322.

20. Bohse J. Acoustic emission characteristics of micro-failure processes in polymer blends and composites. *Compos Sci Technol* 2000; 60: 1213–1226.
21. Haselbach W and Lauke B. Acoustic emission of debonding between fibre and matrix to evaluate local adhesion. *Compos Sci Technol* 2003; 63: 2155–2162.
22. Ramirez-Jimenez CR, Papadakis N, Reynolds N, et al. Identification of failure modes in glass/polypropylene composites by means of the primary frequency content of the acoustic emission event. *Compos Sci Technol* 2004; 64: 1819–1827.
23. Marec A, Thomas JH and Guerjouma R. Damage characterization of polymer-based composite materials: multivariable analysis and wavelet transform for clustering acoustic emission data. *Mech Syst Signal Process* 2008; 22: 1441–1464.
24. Li X, Ramirez C, Hines EL, et al. Pattern recognition of fiber-reinforced plastic failure mechanism using computational intelligence techniques. In: *Neural networks. IEEE world congress on computational intelligence*, Hong Kong, 2008, pp.2340–2345. IEEE.
25. Kostopoulos V, Karapappas P, Loutas T, et al. Interlaminar fracture toughness of carbon fibre-reinforced polymer laminates with nano- and micro-fillers. *Strain* 2011; 47: e269–e282.
26. Scholey JJ, Wilcox PD, Wisnom MR, et al. Quantitative experimental measurements of matrix cracking and delamination using acoustic emission. *Compos Part A: Appl Sci Manufact* 2010; 41: 612–623.
27. Sause MGR, Gribov A, Unwin AR, et al. Pattern recognition approach to identify natural clusters of acoustic emission signals. *Pattern Recogn Lett* 2012; 33: 17–23.
28. Sause MGR and Horn S. Simulation of acoustic emission in planar carbon fiber reinforced plastic specimens. *J Nondestr Eval* 2010; 29: 123–142.
29. Sause MGR and Horn S. Influence of specimen geometry on acoustic emission signals in fiber reinforced composites: FEM-simulations and experiments. In: *Proceedings of the 29th European conference on acoustic emission*, Vienna, Austria, 2010.
30. Sause MGR, Müller T, Horoschenkoff A, et al. Quantification of failure mechanisms in mode-I loading of fiber reinforced plastics utilizing acoustic emission analysis. *Compos Sci Technol* 2012; 72: 167–174.
31. Wilcox PD, Lee CK, Scholey JJ, et al. Progress towards a forward model of the complete acoustic emission process. *Adv Mater Res* 2006; 13–14: 69–75.
32. Sause MR and Horn S. Quantification of the uncertainty of pattern recognition approaches applied to acoustic emission signals. *J Nondestr Eval* 2013; 32: 242–255.
33. Scott AE, Mavrogordato M, Wright P, et al. In situ fibre fracture measurement in carbon-epoxy laminates using high resolution computed tomography. *Compos Sci Technol* 2011; 71: 1471–1477.
34. Mucha P. *Laserbearbeitung von CFK – Bearbeitungsstrategien und mechanische Eigenschaften*. Diplomathesis, Institut für Strahlwerkzeuge (IFSW), Universität Stuttgart, 2011. IFSW 11-20.